

EFFECT OF PURLIN – SHEETING INTERACTION ON THE BUCKLING RESISTANCE OF Z-PURLINS

Mansour Kachichian * - *László Dunai***

ABSTRACT

In this paper a research about the effect of lateral stiffnesses on the buckling resistance of secondary load-bearing systems in roofs is presented. The roof specimens are built from Z-purlin and trapezoidal sheeting connected to each other directly. The interaction is expressed by the lateral stiffness of the purlin-to-sheeting assembly; the stiffness values are obtained from the results of experiments and numerical analyses completed on standard roof specimens. The lateral torsional buckling resistance of roof system can be expressed by the lateral stiffness. The first part of the paper presents the stiffnesses obtained from numerical analyses and their comparison to the results of experiments. In the second part the buckling resistance is studied and analysed on the bases of the parameters of purlin-sheeting system.

1. INTRODUCTION

Typical secondary load-bearing roof systems of industrial-type steel buildings are build-up from cold-formed purlin and sheeting profiles. The typical failure mode of the purlin is the lateral torsional buckling, with distortion of the cross-section. This behaviour is highly affected by the interaction of the purlin and sheeting. The interaction of the two structural elements can be expressed by the lateral stiffnesses of the system. The lateral stiffnesses can be obtained by standardized testing procedure of Eurocode 3 [1]. In this paper these values are obtained from parallel experimental and numerical analyses of 36 test specimens tested in two versions with positive load to study the gravity load effect and with negative load to study the effect of wind uplifting load. The lateral stiffnesses are used in the current study to determine the buckling resistance of the purlins.

The experimental program is published in details in [2] and [3] publications of the authors; the numerical model and analysis is reported in this paper through the comparison made between the experimental results and the numerical ones.

The buckling resistances are determined by the design method of [1], using the experimental results as input parameters. The resistance values are analysed in a parametric study with respect to the following parameters:

- lateral stiffness of purlin-sheeting system;
- spacing of the rigid supports of the free flange of purlins.

* civil engineer, PhD Student, BUTE Dept. of Structural Engineering

** civil engineer, Dr. habil., associate professor, BUTE Dept. of Structural Engineering

2. LATERAL STIFFNESS OF PURLIN-SHEETING INTERACTION

2.1. Lateral stiffness definition

The lateral stiffnesses are obtained from the results of standardized experimental and numerical analyses, as shown in Figure 1. The test models are built-up from Z-purlin with heights of 150, 200 mm and trapezoidal sheeting with 45 mm depth; the two components are connected directly by self-drilling screws. The experimental and numerical specimens are loaded through the free flange and the loads with the corresponding displacements are measured.

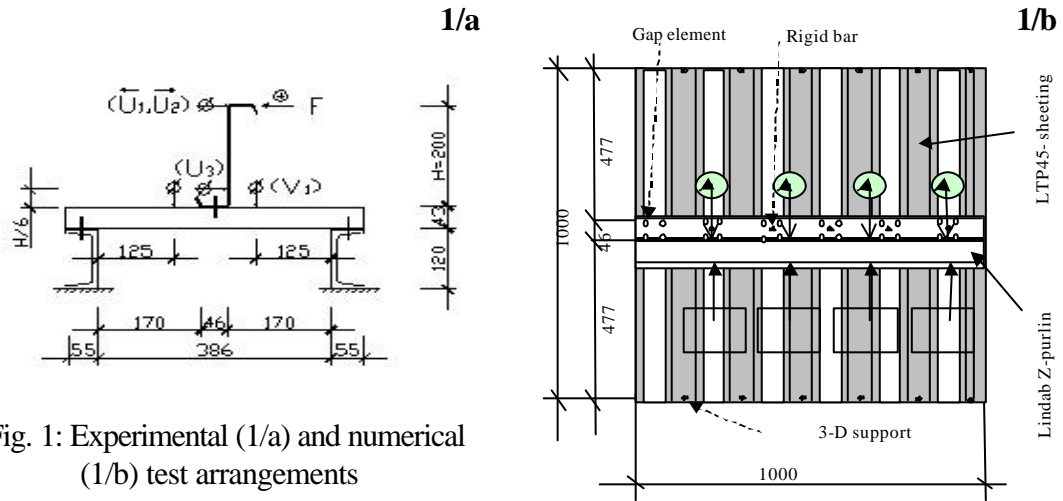


Fig. 1: Experimental (1/a) and numerical (1/b) test arrangements

The lateral stiffness (K) is obtained from Eq. 1, as it is recommended by [1]. In the experimental program the following parameters are used:

- two connection modes,
- Z-purlin with two different heights,
- Z-purlin with three different thicknesses,
- sheeting with three different thicknesses.

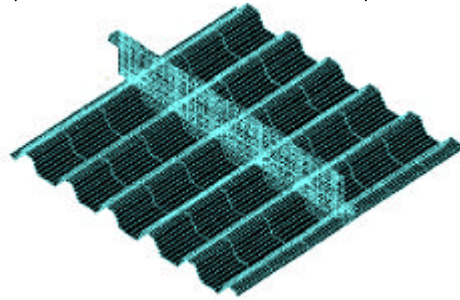


Fig. 2: Numerical model

$$K = \frac{1}{\frac{1}{K_A} + \frac{1}{K_B}} = \frac{F}{d} \quad (1)$$

Where:

- F load per unit length of test specimen to produce a lateral deflection $H/10$,
- H depth of the Z-purlin,
- δ lateral displacement of the top flange in the direction of the load,
- K_A lateral stiffness per unit length corresponding to the rotational stiffness of the connection between the sheeting and the purlin,
- K_B lateral stiffness per unit length due to distortion of the cross-section of the purlin.

2.2. Lateral stiffness values

The experimentally determined lateral stiffnesses are studied in the function of different parameters; the results can be found in [2] and [3]. In parallel the lateral stiffnesses are determined by finite element analyses (K_m), too. Table 1 illustrates the stiffnesses for all the specimens having the smallest thickness of both purlins. (Note: the specimen code is detailed in Table 3).

Table 1: Lateral stiffness-numerical model

Model stiffness for Z-150 purlin					
Specimen code	$K_m * 100$	$K_m * 100$	Specimen code	$K_m * 100$	$K_m * 100$
	[(N/mm)/mm]	[(N/mm)/mm]		[(N/mm)/mm]	[(N/mm)/mm]
	+	-		+	-
Z11-S5/A	0,431	0,578	Z11-S5/B	0,558	0,642
Z11-S6/A	0,551	0,630	Z11-S6/B	0,678	0,801
Z11-S7/A	0,804	0,749	Z11-S7/B	0,759	0,92
Model stiffness for Z-200 purlin					
Specimen code	$K_m * 100$	$K_m * 100$	Specimen code	$K_m * 100$	$K_m * 100$
	[(N/mm)/mm]	[(N/mm)/mm]		[(N/mm)/mm]	[(N/mm)/mm]
	+	-		+	-
Z21-S5/A	0,288	0,387	Z21-S5/B	0,309	0,427
Z21-S6/A	0,386	0,488	Z21-S6/B	0,423	0,554
Z21-S7/A	0,467	0,567	Z21-S7/B	0,525	0,655

The numerical results are compared to the experimental values; the ratio of them is presented in Table 2. From the results it can be seen, that the ratios have a definite tendency: the numerical analysis always overestimates the lateral stiffnesses (in general about 20-30 percentages). It can be also concluded, that the values have a big scatter (from 56 to 97 percentage). These conclusions call the attention on the complex and complicated behaviour of the purlin-sheeting details.

Table 2: Comparison of experimental/numerical stiffnesses

Comparison of Experimental/Model stiffness for Z-150 purlin					
Specimen code	$(K_e/K_m) * 100$	$(K_e/K_m) * 100$	Specimen code	$(K_e/K_m) * 100$	$(K_e/K_m) * 100$
	[%]	[%]		[%]	[%]
	+	-		+	-
Z11-S5/A	84	74	Z11-S5/B	83	81
Z11-S6/A	76	81	Z11-S6/B	77	74
Z11-S7/A	64	84	Z11-S7/B	85	85
Comparison of Experimental Model stiffness for Z-200 purlin					
Specimen code	$(K_e/K_m) * 100$	$(K_e/K_m) * 100$	Specimen code	$(K_e/K_m) * 100$	$(K_e/K_m) * 100$
	[%]	[%]		[%]	[%]
	+	-		+	-
Z21-S5/A	75	97	Z21-S5/B	56	81
Z21-S6/A	59	74	Z21-S6/B	64	63
Z21-S7/A	57	60	Z21-S7/B	62	63

The developed model cannot be used directly for further studies to determine the lateral stiffnesses. From the scatter of the results it is also evident that the numerical model cannot be improved without further parallel experimental and numerical studies.

3. LATERAL BUCKLING DESIGN MODEL

In the Eurocode 3 [1] the lateral buckling formula is based on the elastically supported flexural buckling design model of free flange of Z-purlin, as it is given by (Eq. 2), and illustrated in Figure 3. In the checking the effects of the flexural buckling and the transverse bending due to torsion of the free flange are combined.

$$\left[\frac{1}{c} * \left(\frac{M_{y,Sd}}{W_{eff,y}} + \frac{N_{Sd}}{A_{eff}} \right) + \frac{M_{fz,Sd}}{W_{fz}} \right] \leq \frac{f_{yb}}{g_{M1}} \quad (2)$$

Where:

- c** reduction factor for flexural buckling of the free flange,
- $M_{y,Sd}$ in plane bending design moment,
- N_{Sd} axial force,
- f_{yb} yield strength of the profile material,
- g_{M1} partial safety factor,
- $M_{fz,Sd}$ bending moment in the free flange due to the lateral load $k_h * q_{FD}$,
- A_{eff} effective area of the cross-section for uniform compression,
- $W_{eff,y}$ effective section modulus of the cross-section for bending about the y-y axis,
- W_{fz} gross elastic section modulus of the free flange plus 1/6 of the web height, for bending about the z-z axis.

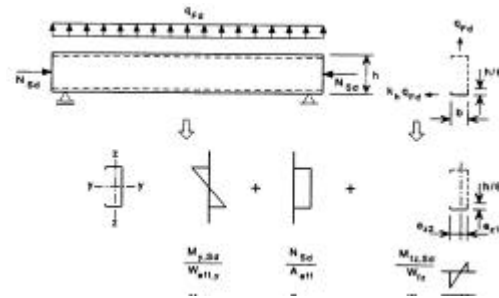


Fig. 3: Buckling formula components

In case of gravity or uplift load a lateral distributed force is generated in positive or negative senses, respectively (the uplift equivalent load is the negative one in our models as it is shown in Figure 1). The deformations caused by uplift loads are shown with superposition of the deformation components in Figure 4. It can be seen in the figure, that the lateral deformation is caused by the rigid body type rotation of the purlin-sheeting system and the distortional deformation of the purlin web.



Fig. 4: Components of deformations from uplift load

The buckling resistance factor can be determined from the unsupported length of the free flange. It is dependent on the length of the compression region for different statical models and types of loading. Figure 5 illustrates the definition of the compression zones for uplift loading for simply supported and continuous statical models, respectively.

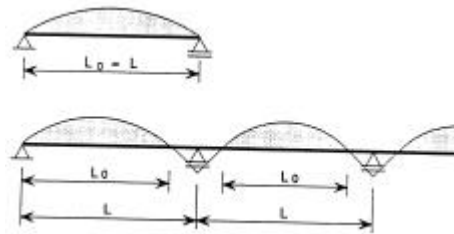


Fig. 5: Length of the compression region

4. BUCKLING RESISTANCE DEFINITION

4.1. General

In the further part of the paper we analyse the effect of the lateral stiffness of the purlin-sheeting system on the buckling resistance. In the calculations we use the standardized formulation, inserting in it the experimental lateral stiffness results as input parameters. In the design model we use pure bending, eliminating the effect of the axial force and the torsion. By these assumptions, rearranging the design formula of (Eq. 2) the buckling resistance can be obtained for the studied sets of parameters.

4.2. Buckling resistance

Having the assumptions of Section 4.1 the buckling resistance of the purlin can be expressed as follows:

$$M_{y,Rd} = c * W_{eff,y} \frac{f_{yb}}{g_{ML}} \quad (3)$$

Where: $W_{eff,y}$ effective section modulus,
 c buckling reduction factor; in the function of \bar{I} and f .
 \bar{I} relative slenderness of the free flange, as an elastically supported compression member: $\bar{I} = \bar{I}_{fz}$;

$$f = 0.5 \left[1 + a(\bar{I} - 0.2) + \bar{I}^2 \right] \quad (4)$$

The formulation of the slenderness is the following:

$$\bar{I}_{fz} = \frac{l_{fz}/i_{fz}}{I_1} \quad (5)$$

$$I_1 = p \sqrt{\frac{E}{f_{yb}}} \quad (6)$$

$$l_{fz} = 0.7l_0 \left(1 + 13.1R_0^{1.6} \right)^{-0.125} \quad (7)$$

$$R_0 = \frac{Kl_0^4}{p^4 EI_{fz}} \quad 0 \leq R_0 \leq 200 \quad (8)$$

$$l_0 = 0.85l \quad (9)$$

$$i_{fz} = \sqrt{\frac{I_{fz}}{A_{fz}}} \quad (10)$$

Where:

- l rigid support span;
- l_0 length of the compression region of the free flange (shown in Fig. 5);
- i_{fz} radius of gyration of the free flange for bending about z-z;
- l_{fz} buckling length of the free flange;
- I_{fz} second moment of area of the gross cross-section of the free flange plus 1/6 of the web height for bending about z-z axis;
- A_{fz} area of the gross cross-section of the free flange plus 1/6 of the web height;
- K lateral stiffness per unit length obtained from experiments;
- E elastic modulus.

5. PARAMETRIC STUDY

5.1. Studied parameters

In this paragraph the different parameters used to build the tested specimens are presented taking all the combinations of 6 types of purlin, and 3 types of sheeting connected by 2 connection modes as it is presented in Table 3.

Table 3: The characteristics of the specimens

Z-purlins			LTP45-sheeting		SD6 self-drilling screws	
Height [mm]	Thickness [mm]	Notations	Thickness [mm]	Notations	Screws per sheet width	Notations
150	1.0	Z11	0.5	S5	3	A
150	1.5	Z12	0.6	S6	5	B
150	2.0	Z13	0.7	S7		
200	1.2	Z21				
200	1.5	Z22				
200	2.0	Z23				

5.2. Results

The lateral stiffnesses are calculated for 36 specimens as mentioned in Chapter 2. Then the buckling resistance are determined as it is shown in Chapter 4 for all specimens in 7 versions of support spacing in addition to yielding moment determination. From these results, 12 illustrating example are presented in Table 4 taking Z11 and Z21 purlins with all sheeting combinations and both connection modes.

5.3. Evaluation the results

The evaluation of the buckling resistance of specimens is expressed by comparisons. These comparisons are illustrated in percentage compared to Z23 yielding moment in Fig. 6/A, B; presenting specimens with Z-150 purlins with all the combinations to the B version of connection in Fig. 6/A; and specimens with Z-200 purlins with all the combinations to the A version of connection in Fig. 6/B. Then the

comparisons are taken with respect to spacing and lateral stiffnesses for all specimens having S6 sheeting in case of Z150 purlin in Fig. 7/A, and for all specimens having S7 sheeting in case of Z-200 purlin in Fig. 7/B.

Table 4: Buckling resistance for different spans

Specimen codes	Negative $K_e * 100$ [(N/mm)/mm]	$W_{eff,y} * f_y / 1.1$ [kN*m]	$M_{y, sd}$ [kN*m]						
			L=1	L=2	L=3	L=4	L=5	L=6	L=7
Z11-S5/A	0.43	2.37	2.23	1.78	1.35	1.19	1.11	1.04	0.99
Z11-S6/A	0.51	2.37	2.23	1.79	1.4	1.25	1.16	1.1	1.05
Z11-S7/A	0.63	2.37	2.23	1.8	1.46	1.32	1.24	1.17	1.12
Z21-S5/A	0.31	4.47	4.2	3.31	2.28	1.89	1.72	1.61	1.52
Z21-S6/A	0.31	4.47	4.2	3.30	2.28	1.88	1.71	1.6	1.52
Z21-S7/A	0.32	4.47	4.2	3.31	2.28	1.89	1.72	1.61	1.52
Z11-S5/B	0.52	2.37	2.23	1.79	1.4	1.26	1.17	1.1	1.05
Z11-S6/B	0.59	2.37	2.23	1.8	1.44	1.3	1.22	1.15	1.1
Z11-S7/B	0.78	2.37	2.23	1.81	1.52	1.4	1.32	1.25	1.19
Z21-S5/B	0.36	4.47	4.2	3.31	2.33	1.96	1.79	1.68	1.59
Z21-S6/B	0.35	4.47	4.2	3.31	2.32	1.95	1.78	1.66	1.58
Z21-S7/B	0.42	4.47	4.2	3.32	2.39	2.04	1.88	1.76	1.67

The parameters affecting the buckling resistance of specimens can be categorised in the following four points:

- Purlin thickness effect: each of the three groups seen in each of Fig. 6/A and B belongs to one purlin thickness, what shows the dominant effect of purlin thickness.
- Sheeting thickness effect: the separation after 2 m spacing in each group mentioned above, shows the sheeting thickness effect; this effect is about 2% for weak purlins and 5% for stronger ones, and it seen is as well that this effect vanishes after 4 m support distance.
- Rigid support spacing effect: it is clearly seen in Fig. 6, that the buckling resistance decreases by the increment of the supported distance. The reduction for 7 m supported length in case of specimens having Z150 purlins is about 50%, while it is about 65% for specimens having Z200 purlins.
- Purlin height effect: The higher the purlin the bigger the reduction in the buckling resistance of specimens as it can be seen from Fig.6/A and B.

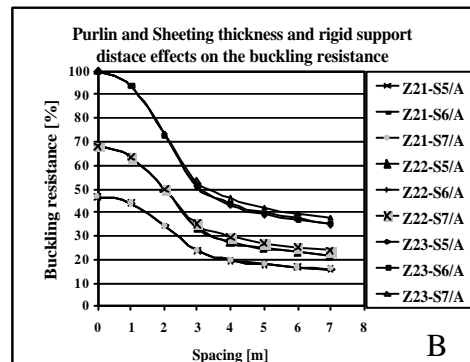
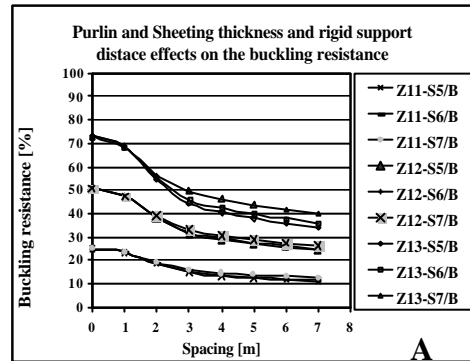


Fig. 6: Buckling resistance

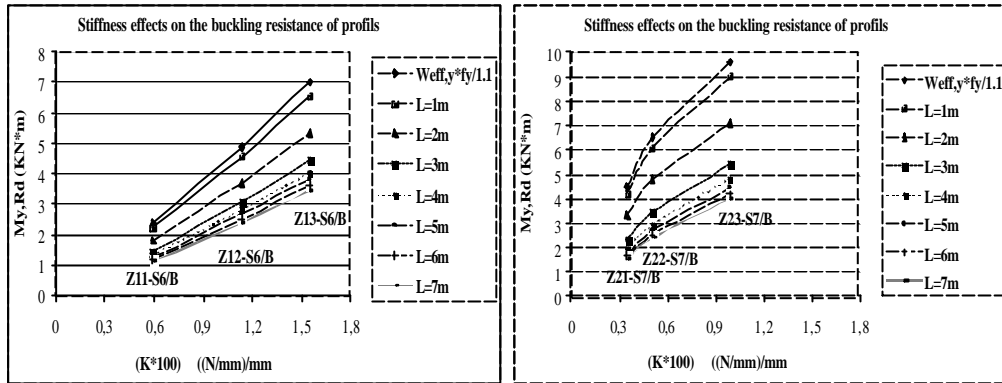


Fig. 7: Effect of span and lateral stiffness on the buckling resistance

6. CONCLUDING REMARKS

In this paper, the effect of purlin-sheeting interaction on the purlin resistance is investigated. The research is not finished yet, at the current level the following concluding remarks can be done.

From the numerical and experimental studies on lateral spring stiffness of the purlin-sheeting assembly it can be clearly seen that the lateral stiffness cannot be obtained from the developed numerical model directly. The development of the model requires further parallel experimental and numerical studies.

The experimentally determined lateral stiffness is used to calculate the buckling resistance of the purlin, supported only on one flange. The results show, that the relationship of the spring stiffness and buckling resistance is almost linear for the studied parameters, independently from the spans. In the research the roles of the different parameters of the structural details on the resistance are determined. It is found that significant changes in the resistance are obtained between the spans of 2 - 3 meters.

ACKNOWLEDGEMENT

The authors acknowledge the support of Lindab Ltd. and OTKA T035147 project.

REFERENCES

- [1] ENV 1993-1-3, Eurocode 3, Design of Steel Structures, Part 1.3: Cold Formed Thin-Gauge Members and Sheeting, 1996.
- [2] Kachichian M.- Dunai L.- Kaltenbach L.- Kálló M.: Experimental study on the interaction of steel sheeting and Z-purlins. *6th Int. Coll. on Stability and Ductility of Steel Structures, Timisoara*, Eds. Dubina D, Iványi M., Elsevier, pp 293-306, 1999.
- [3] Kachichian M.- Dunai L.- Kaltenbach L.- Kálló M.: *Interaction of LINDAB Z-purlins and LTP45-sheetings*, Department Report, BUTE, Budapest, 1998.